Self-organized propagation of dislocations in GaN films during epitaxial lateral overgrowth

Akira Sakai[a)]
Fundamental Research Laboratories, NEC Corporation, 34 Miyukigaoka, Tsukuba, Ibaraki 305-8501, Japan

Haruo Sunakawa, Akitaka Kimura, and Akira Usui
Optoelectronics and High Frequency Device Research Laboratories, NEC Corporation, 34 Miyukigaoka, Tsukuba, Ibaraki 305-8501, Japan

(Received 26 April 1999; accepted for publication 29 November 1999)

Dislocation propagation and defect evolution in GaN films formed by epitaxial lateral overgrowth (ELO) are examined by transmission electron microscopy. A novel effect that induces self-organized propagation of preexisting dislocations in ELO films is evaluated. This propagation forms dislocations into bundle structures along the stripes of masks used for ELO. The dislocation bundling gives rise to crystallographic tilting in the overgrown region on the mask and leads to a total reduction of threading dislocation density in the film. © *2000 American Institute of Physics.* [S0003-6951(00)04504-6]

Epitaxial GaN films are attractive as substrate materials for blue-light-emitting diodes and laser diodes as well as high-power electronic devices. Much attention has been directed to growing the films with low threading dislocation densities.[1] Epitaxial lateral overgrowth (ELO) has proved to be a powerful technique for reducing the threading dislocation density in various semiconductor films.[1] In order to improve such a dislocated GaN film texture, ELO using hydride vapor phase epitaxy (HVPE)[2,3] and metalorganic vapor phase epitaxy (MOVPE)[4,5] has been demonstrated. We have revealed by transmission electron microscopy (TEM) the structures of dislocations in HVPE–ELO films[6] and the structures of characteristic defects causing tilting of the *c* axis in the overgrown region of those films.[7]

Crystallographic tilting, in other words, *bending* of the overgrown film, is recognized to be a common problem in various ELO films since it often occurred in other GaN films.[8,9] Although appropriate characterizations of the film structures have been previously achieved in these cases, understanding of the relationship between the microstructures in the overgrown region and the defect morphology in the window region is still not satisfactory. In this letter, through TEM analysis of ELO–GaN films formed under various conditions, we clarify a novel effect of ELO that gives rise to *self-organized propagation* of dislocations coming from the window region. This propagation induces the crystallographic tilting in the overgrown region and eventually leads to the reduction of threading dislocation density in the film.

The substrate used in this experiment was a 1-μm-thick GaN layer grown by MOVPE on a sapphire (0001) wafer with the SiO_2 mask/window stripes along either the $\langle 11\bar{2}0\rangle$ or the $\langle 1\bar{1}00\rangle$ directions of the GaN surface. ELO was performed using either HVPE or MOVPE. The other experimental details are available elsewhere.[2,5,6]

We first look at the characteristic of defect morphology in ELO films. In this study, we performed extensive TEM observations on four types of films that were categorized by alternative mask directions ($\langle 11\bar{2}0\rangle$ or $\langle 1\bar{1}00\rangle$) and growth methods (HVPE or MOVPE). Although details were slightly different from sample to sample, we consequently found that the $\langle 11\bar{2}0\rangle$ HVPE, $\langle 1\bar{1}00\rangle$ HVPE, and $\langle 11\bar{2}0\rangle$ MOVPE samples had a common feature of defect morphology. We, therefore, review here the $\langle 11\bar{2}0\rangle$ HVPE sample[6,7] shown in Fig. 1 as a representative of the others. One typical feature is angled dislocations; for example, denoted by type A. They originate from threading edge dislocations with a Burgers vector of $\mathbf{b}=1/3\langle 11\bar{2}0\rangle$ type that are the majority in the substrate. The other feature is characterized by tilt boundaries formed in the overgrown region, denoted by D1 and D2. In each boundary, the composing dislocations with the same Burgers vector run along the mask stripe and pile up approximately along the $\langle 0001\rangle$ direction. Since the sign of their Burgers vector is opposite to each other, i.e., the dislocation corresponds to the upper (lower) edge of the extra-half plane in the D1 (D2) defect, the *c* axes of two overgrown regions separated by the defects tilt toward the center of the mask with respect to the window region.

Next, in order to elucidate the relationship between the dislocation propagation and the tilt boundary formation, we examine ELO films at the intermediate stage in the lateral overgrowth on the mask. Figure 2(a) is a typical cross-sectional TEM image near the overgrown region of the $\langle 11\bar{2}0\rangle$ HVPE sample. It is observed that dislocations, identical to type B as defined in Ref. 7, intersected with a $\{1\bar{1}01\}$ facet appearing during the lateral overgrowth. Note that many end-on dislocations parallel to the $[11\bar{2}0]$ direction were observed with some of them laying on top of each other

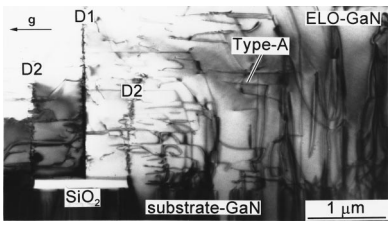

FIG. 1. Cross-sectional TEM image with $\mathbf{g}=1\bar{1}00$ near the ELO-film/substrate-GaN interface in the $\langle 11\bar{2}0\rangle$ HVPE sample.

[a)]Present address: Department of Crystalline Materials Science, Graduate School of Engineering, Nagoya University, Furo-cho, Chikusa-ku, Nagoya 464-8603, Japan; electronic mail: sakai@alice.xtal.nagoya-u.ac.jp

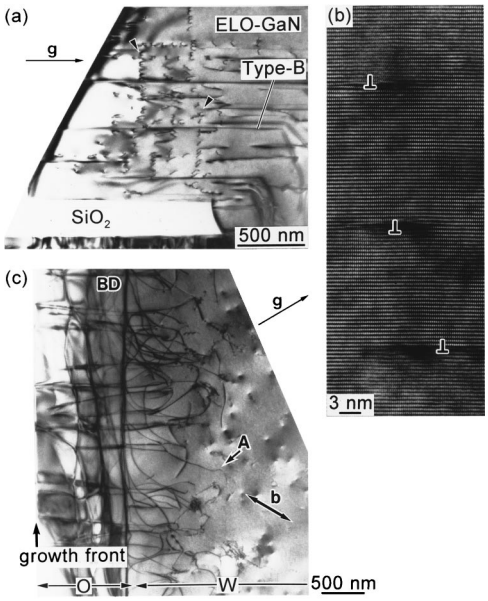

FIG. 2. (a) Cross-sectional TEM image with $\mathbf{g}=\bar{1}100$ showing dislocations in the $\langle 11\bar{2}0\rangle$ HVPE–ELO film at the intermediate stage in lateral overgrowth. (b) Cross-sectional high-resolution image of the end-on dislocations in the same sample. (c) Plan-view image with $\mathbf{g}=\bar{2}110$ of the overgrown (*O*) and the window (*W*) regions in the same sample. **b** denotes its Burgers vector direction.

at nearly regular separations along the [0001] direction, as indicated by arrowheads in Fig. 2(a). Individual structures observed through the $[11\bar{2}0]$ projection of the end-on dislocations were directly determined from their high-resolution TEM images, as in the example shown in Fig. 2(b). As a result, we found that every end-on dislocation observed in the sample had its extra-half plane pointing towards the film surface, as denoted by $\perp$ in Fig. 2(b). Such structures and their regular arrangement are quite similar to those of the D2 defect shown in Fig. 1.

Figure 2(c) shows a plan-view TEM image of the same sample. Here we notice two types of distinguishable dislocation morphology as well as type-B dislocations that propagate approximately normal to the mask stripe. First, we observed a bundle of dislocations, denoted by BD along the mask stripe in the overgrown region, corresponding to the end-on dislocations seen in Fig. 2(a). Second, dislocations propagated from the window regions to the bundle can be seen, for example, indicated by arrow A. We analyzed the systematic contrast variation of the dislocations and found that they were type-A dislocations with Burgers vector of $\mathbf{b}=\langle 11\bar{2}0\rangle$ type. These results unambiguously show that type-A dislocation segments parallel to the *c* plane of GaN, which come from the window regions, propagated along the mask stripe direction and formed into a bundle in the overgrown region.

It is now clear from the earlier results that self-organized propagation of type-A dislocations resulted in the bundle consisting of dislocations with an identical sign of Burgers vector. Since their Burgers vector on the prismatic plane of the hexagonal crystal simultaneously lies on the basal *c* plane and, as reported previously,[6] their lateral segments initially propagate parallel to their Burgers vector, it is plausible that the lateral screw segments readily cross-slip onto the *c* plane. However, we observed no such dislocation bundling in the

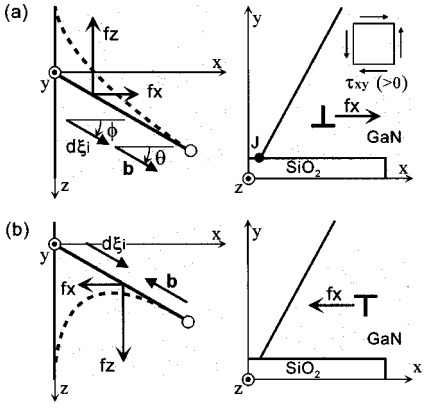

FIG. 3. Schematic representation of type-A dislocation movement on the *c* plane by the forces under the positive τ_{xy} condition in plan-view (left) and cross-sectional view (right). The definition of the sign of Burgers vector that determines the position of the extra-half plane follows that given in Ref. 12. Directions of the forces ($|\mathbf{f}_x|=\sqrt{3}b\tau_{xy}/4$ and $|\mathbf{f}_z|=3b\tau_{xy}/4$) are indicated by the arrows. Two cases are shown in which the directions of Burger vector **b** and a unit vector of the dislocation line $d\boldsymbol{\xi}_i$ are (a) identical and (b) opposite to each other. The dislocations before and after being forced to move are described by solid and broken lines, respectively. Note the direction of the positive τ_{xy}.

samples at the growth stage before starting overgrowth, and type-A dislocations had only a tendency to propagate along its Burgers vector to the growth front. Furthermore, in general, dislocation lines tend to follow the direction of minimum energy per unit growth length.[10,11] Hence, there must be an external force for promoting type-A dislocations to propagate along the mask stripe direction during the lateral overgrowth. Using the Peach–Koehler's equation,[12] we derive the force exerted in the unit length on type-A dislocations lying on the *c* plane of the ELO–GaN film on the mask. Figure 3 shows a film with the *z* axis parallel to the mask stripe direction and the *y* axis parallel to the *c* axis of GaN immersed in the stress field: Type-A dislocations lie in the *x*-*z* plane with **b** and $d\boldsymbol{\xi}_i$ (a unit vector of a line element of the dislocation) at an angle θ and ϕ with respect to the *x* axis, respectively. The fact that the scale of the crystal in the mask stripe direction is much larger than those in the other orthogonal directions allows us to postulate a plane-strain state for the stress field described by symmetric three-dimensional tensor.[13] In terms of unit vectors **i**, **j**, and **k** for the *x*, *y*, and *z* axes, respectively, the force $\mathbf{f}_A$ is then given by

$$\mathbf{f}_A=(b\cos\theta\sin\phi\tau_{xy})\mathbf{i}+(b\sin\theta\cos\phi\sigma_{zz}-b\cos\theta\sin\phi\sigma_{xx})\mathbf{j}+(-b\cos\theta\cos\phi\tau_{xy})\mathbf{k}, \quad (1)$$

where τ_{xy} is shear stress acting perpendicularly to the *z* axis and $\sigma_{xx}(\sigma_{zz})$ is normal stress acting along the *x* axis (*z* axis). The first and third terms of Eq. (1), respectively, describe the forces exerted along the *x*- and *z*-axis directions ($\mathbf{f}_x$ and $\mathbf{f}_z$) and, thus, the resultant force of $\mathbf{f}_x$ and $\mathbf{f}_z$ causes dislocation movement on the *x*-*z* plane. We emphasize in this expression that the glide motion of type-A dislocations on the *c* plane is principally determined by the shear stress τ_{xy} acting perpendicularly to the mask stripe direction.

From our earlier result that type-A dislocation with $\mathbf{b}=1/3\langle 11\bar{2}0\rangle$ has a screw character on the *c* plane,[6] we assume an initial morphology (before the force acts) in the ELO film where the dislocation, with **b** and $d\boldsymbol{\xi}_i$ both making an angle of 30° with respect to the *x* axis, emerges at the

growth front. Figures 3(a) and 3(b) are a plan-view and a cross-sectional view along the mask stripe that illustrate $\mathbf{f}_x$ and $\mathbf{f}_z$ under *positive* τ_{xy} condition when the Burgers vector is opposite. As shown in Fig. 3(a), the dislocation with its extra-half plane pointing towards the film surface (hereafter we define as a positive dislocation) is forced to move along the positive x and negative z directions so that ϕ increases. This corresponds to the movement from the growth front toward the inside of the crystal in the cross-sectional view. On the other hand, as shown in Fig. 3(b), the dislocation pointing towards the film/substrate interface (a negative dislocation) is forced to move in the opposite direction to the above case so that ϕ decreases. In the cross-sectional view for this case, the dislocation initially seems to move out of the crystal as ϕ decreases from positive to zero and then emerges as the positive dislocation and moves toward the inside of the crystal as ϕ increases negatively. This model well explains essential factors of the self-organized propagation where the positive and the negative type-A dislocations randomly distributed form into a bundle structure consisting only of positive dislocations along the mask stripe.

It is obvious that such distribution of positive dislocations causes a bending of the overgrown region so that the c axis tilts toward the center of the mask. We, therefore, ought to deduce the origin of the force that induces the positive τ_{xy}. It is reasonable to assume that the force acting on the GaN crystal comes from the interface between the overgrown region and the SiO_2 mask. In our MOVPE samples, densification of the SiO_2 mask was apparently observed. But no thickness and width variations of the mask depending on the growth period were observed in the HVPE samples, meaning that etching or densification of the mask did not occur during ELO. Nevertheless, the c-axis tilting was clearly observed in both samples. This implies that the volume change of the mask is less effective to induce the bending. Another possible origin is capillary stress applied during overgrowth.[8] In principle, the capillary stress is caused by an imbalance among three interface tensions acting at a triple junction [see point J in Fig. 3(a)] of a GaN $\{1\bar{1}01\}$ facet, a SiO_2 mask surface and a GaN/SiO_2 interface. One typical example is the case in which compressive stress is applied perpendicularly to the stripe direction along the GaN/SiO_2 interface. This would be mainly induced by a large GaN/SiO_2-interface tension. From analytical calculations based on elasticity theory[13] for the film having the geometry shown in Fig. 3, we found that the compressive stress gave rise to positive τ_{xy} values in the vicinity of the growth front with the $\{1\bar{1}01\}$ facet. Furthermore, we experimentally proved that the tilt angle of the c axis increases when increasing mask width and depended sensitively on the shape of the growth front during overgrowth.[5] These results strongly suggest that the force determined by the imbalance of the interface tensions transformed the microstructure of the overgrown region. The capillary stress, therefore, seems to be the most probable candidate for the origin of the force.

Equation (1) clearly shows that force cannot be exerted on dislocations running along the c axis. In fact, we rarely observed a self-organized morphology in the $\langle 1\bar{1}00\rangle$ MOVPE samples containing noticeably fewer lateral dislocations in the window region than those in the other three types of samples. Although Ref. 8 showed such morphology, the amount of dislocations was low compared with that in the other types of samples.

As a result of our findings, we can obtain the following scenario for the defect formation accompanying the c-axis tilting in the overgrown region during ELO. The film containing the lateral segments of type-A dislocations overgrows on the mask while being stressed. The stress induces a force exerted on type-A dislocations on the c plane so that self-organized propagation along the mask stripe occurs. The resultant positive dislocations in the overgrown region are the origin of the D2 defect. Then, negative dislocations are formed at the coalesced site partly by the reverse propagation of positive dislocations such that the bending caused by their arrangement can be accommodated. This corresponds to the formation of a tilt boundary in the D1 defect near the center of the mask. Final arrangement for the D2 defect is determined by an interaction among the positive dislocations in the stress field of the coalesced film. Typically, in the case of the $\langle 11\bar{2}0\rangle$ mask, all dislocations have a mixed character. So they form an energetically stable arrangement, i.e., piling up straight along the c axis, by the interactive forces due to their edge component as well as by either attractive or repulsive forces (depending on the direction of the screw term) due to their screw component. From this point of view, a kind of ''polygonization'' [10] might occur in the overgrown region during ELO. Hence, we observe this phenomenon as the D2 defect having a complete form of a tilt boundary in Fig. 1 and as the partially arranged dislocations in Fig. 2.

In summary, we have evaluated a novel effect of ELO that reduces threading dislocation density in the film. The mask induces self-organized propagation of the preexisting dislocations that distributes the dislocations into bundles along the mask. This bundling effect plays a crucial role in suppressing the vertical propagation of the dislocations.

[1] Y. Ujiie and T. Nishinaga, Jpn. J. Appl. Phys., Part 2 **28**, L337 (1989); K. Kato, T. Kusunoki, C. Takenaka, T. Takahashi, and K. Nakajima, J. Cryst. Growth **115**, 174 (1991).
[2] A. Usui, H. Sunakawa, A. Sakai, and A. A. Yamaguchi, Jpn. J. Appl. Phys., Part 2 **36**, L899 (1997).
[3] K. Hiramatsu, H. Matsushima, T. Shibata, N. Sawaki, K. Tadamoto, H. Okagawa, Y. Ohuchi, Y. Honda, and T. Matsue, Mater. Res. Soc. Symp. Proc. **482**, 257 (1998).
[4] D. Kapolnek, S. Keller, R. Vetury, R. D. Underwood, P. Kozodoy, S. P. DenBaars, and U. K. Mishra, Appl. Phys. Lett. **71**, 1204 (1997); O. H. Nam, M. D. Bremser, T. S. Zheleva, and R. F. Davis, *ibid.* **71**, 2638 (1997); S. Nakamura, M. Senoh, S. Nagahama, N. Iwasa, T. Yamada, T. Matsushita, H. Kiyoku, Y. Sugimoto, T. Kozaki, H. Umemoto, M. Sano, and K. Chocho, *ibid.* **72**, 211 (1998).
[5] A. Usui, H. Sunakawa, N. Kuroda, A. Kimura, A. Sakai, and A. A. Yamaguchi, *Proceedings of the 2nd International Symposium on Blue Laser and Light Emitting Diodes* (Ohmsha, Tokyo, 1998), p. 17.
[6] A. Sakai, H. Sunakawa, and A. Usui, Appl. Phys. Lett. **71**, 2259 (1997).
[7] A. Sakai, H. Sunakawa, and A. Usui, Appl. Phys. Lett. **73**, 481 (1998).
[8] H. Marchand, X. H. Wu, J. P. Ibbetson, P. T. Fini, P. Kozodoy, S. Keller, J. S. Speck, S. P. DenBaars, and U. K. Mishra, Appl. Phys. Lett. **73**, 747 (1998).
[9] K. Tsukamoto, W. Taki, N. Kuwano, K. Oki, T. Shibata, N. Sawaki, and K. Hiramatsu, *Proceedings of the 2nd International Symposium on Blue Laser and Light Emitting Diodes* (Ohmsha, Tokyo, 1998), p. 488.
[10] J. P. Hirth and J. Lothe, *Theory of Dislocations* (Krieger, Florida, 1992).
[11] H. Klapper, Y. M. Fishman, and V. G. Lutsau, Phys. Status Solidi A **21**, 115 (1974).
[12] M. Peach and J. S. Koehler, Phys. Rev. **80**, 436 (1950).
[13] S. P. Timoshenko and J. N. Goodier, *Theory of Elasticity* (McGraw-Hill, New York, 1970).